

Appendix A

A *CP* Violation Primer

A.1 Generalities

CP violation is defined as a difference in probability between a particle process from the antiparticle process, e.g., between $B \rightarrow f$ and $\bar{B} \rightarrow \bar{f}$. As is typical in quantum phenomena, it requires the presence of two interfering amplitudes. However, besides the familiar i from quantum mechanics, it needs *complex dynamics* as well.¹ That is, the interference involves the presence of two different kinds of phases. Let us elucidate how CPV occurs.

Consider the amplitude $A = A_1 + A_2$ for the particle process, which is a sum of two terms, where amplitude A_j has both a *CP*-invariant phase δ_j (quantum mechanical i) and a CPV phase ϕ_j (i from CPV *dynamics*). Absorbing an overall phase by defining $A_1 = a_1$ to be real, one has

$$\begin{aligned} A &= A_1 + A_2 = a_1 + a_2 e^{i\delta} e^{+i\phi} \\ \bar{A} &= \bar{A}_1 + \bar{A}_2 = a_1 + a_2 e^{i\delta} e^{-i\phi}, \end{aligned} \tag{A.1}$$

where $a_2 \equiv |A_2|$. The δ and ϕ are called the “strong” and “weak” phases, respectively. The strong phase δ arises from (re)scattering or quantum time evolution and does not distinguish between particle and antiparticle, hence the sign is unchanged between A and \bar{A} . However, the dynamical or weak phase ϕ changes sign for the antiparticle process \bar{A} . This enrichment of quantum interference leads to a possible asymmetry between particle and antiparticle probabilities, for example, involving \bar{B}^0 vs. B^0 . From (A.1), one finds

$$\mathcal{A}_{\text{CP}} \equiv \frac{\Gamma_{\bar{B}^0 \rightarrow \bar{f}} - \Gamma_{B^0 \rightarrow f}}{\Gamma_{\bar{B}^0 \rightarrow \bar{f}} + \Gamma_{B^0 \rightarrow f}} = \frac{2a_1 a_2 \sin \delta \sin \phi}{a_1^2 + a_2^2 + 2a_1 a_2 \cos \delta \cos \phi}, \tag{A.2}$$

¹ Imagine e of electrodynamics is complex. This is not possible as it is a gauge coupling.

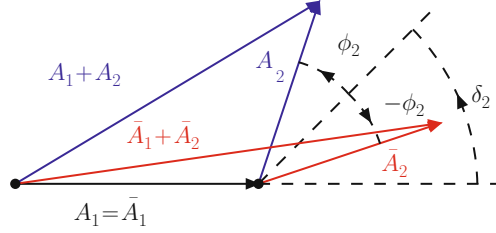


Fig. A.1 Mechanism for CPV, the geometric picture for (A.2)

defined with respect to quarks (e.g., \vec{B}^0 contains a b quark). As \mathcal{A}_{CP} vanishes with either δ or $\phi \rightarrow 0$, CPV requires the presence of *both* CP conserving *and* CPV phases.

Equation (A.1) is illustrated in Fig. A.1, which shows geometrically how the \mathcal{A}_{CP} of (A.2) materializes. By a phase choice, we place $A_1 = \bar{A}_1$ on the real axis. Then A_2 and \bar{A}_2 , which are of the same length $|A_2| = |\bar{A}_2| = a_2$, are as depicted, where A_2 (\bar{A}_2) is rotated by $+\phi$ ($-\phi$) from the common δ phase angle. We see that, if $\delta = 0$, then $A_1 + A_2$ and $\bar{A}_1 + \bar{A}_2$ are at an angle ϕ above or below the real axis and are of equal length. If, however, $\phi = 0$, then $A_1 + A_2$ and $\bar{A}_1 + \bar{A}_2$ coalesce into the same vector, hence are necessarily of equal length. Only when *both* $\delta \neq 0$ and $\phi \neq 0$, do we have $|A_1 + A_2| \neq |\bar{A}_1 + \bar{A}_2|$, as one can see from the asymmetry formula (A.2).

CP Violation in Standard Model with Three Generations

In the KM model with three generations, one needs the presence of all three generations in a process to make CPV occur [1]. In the standard phase convention [2, 3] of keeping V_{us} and V_{cb} real, the unique CPV phase is placed in the 13 element V_{ub} and hence the 31 element V_{td} as well by unitarity of V . We give the CKM matrix V in Wolfenstein form [2–4],

$$V = \begin{pmatrix} V_{ud} & V_{us} & V_{ub} \\ V_{cd} & V_{cs} & V_{cb} \\ V_{td} & V_{ts} & V_{tb} \end{pmatrix} \simeq \begin{pmatrix} 1 - \lambda^2/2 & \lambda & A\lambda^3(\rho - i\eta) \\ -\lambda & 1 - \lambda^2/2 & A\lambda^2 \\ A\lambda^3(1 - \rho - i\eta) & -A\lambda^2 & 1 \end{pmatrix}, \quad (\text{A.3})$$

where,

$$\lambda \equiv V_{us} \simeq 0.22, \quad A\lambda^2 \equiv V_{cb} \simeq 0.04, \quad A\lambda^3\sqrt{\rho^2 + \eta^2} \equiv |V_{ub}| \sim 0.003. \quad (\text{A.4})$$

For those with any interest in flavor and CPV physics, it is useful to memorize (A.3) and the orders of magnitude in (A.4). The current measured strength of the CPV phases $\phi_3 \equiv \arg V_{ub}^*$ and $\phi_1 \equiv \arg V_{td}$ (Belle notation for phases) can be found in Chap. 1.

The matrix V is unitary, i.e.,

$$V^\dagger V = V V^\dagger = I. \quad (\text{A.5})$$

It can be readily checked that this relation holds for the Wolfenstein form of V in (A.3) to λ^3 order. At this order, V_{ts} is real and negative, but it picks up a tiny imaginary part at λ^4 order (see below). Note that $\sqrt{\rho^2 + \eta^2} \sim 1/3$ compared with $\lambda \cong 0.22 \sim 1/4.5$. Thus, together with $A \sim 0.8$, $|V_{ub}|$ is actually closer to λ^4 rather than λ^3 order, while $|V_{td}|$ is of order λ^3 .

Since we highlight CPV in $b \rightarrow s$ and $b \leftrightarrow s$ ($B_s^0 - \bar{B}_s^0$ oscillations) transitions as the current frontier for probing physics beyond SM, we extend (A.3) to λ^5 order,

$$V \cong \begin{pmatrix} 1 - \frac{1}{2}\lambda^2 - \frac{1}{8}\lambda^4 & \lambda & A\lambda^3(\rho - i\eta) \\ -\lambda + A^2\lambda^5(\frac{1}{2} - \rho - i\eta) & 1 - \frac{1}{2}\lambda^2 - (\frac{1}{8} + \frac{1}{2}A^2)\lambda^4 & A\lambda^2 \\ A\lambda^3(1 - \bar{\rho} - i\bar{\eta}) & -A\lambda^2 + A\lambda^4(\frac{1}{2} - \rho - i\eta) & 1 - \frac{1}{2}A^2\lambda^4 \end{pmatrix}, \quad (\text{A.6})$$

where the definitions of (A.4) for the three upper-right off-diagonal elements, namely V_{us} , V_{cb} , and V_{ub} , remain the same and [2, 3] $\bar{\rho}/\rho = \bar{\eta}/\eta = 1 - \frac{1}{2}\lambda^2$. We see that $V_{ts}^* V_{tb}$ picks up a CPV phase at λ^4 order, while the real part is at λ^2 order. This implies a rather small phase angle, as compared with the phase in $V_{td}^* V_{tb}$, where the imaginary and real parts are not drastically different in strength.

It is useful to visualize the so-called unitarity triangles that arise from the unitarity relation (A.5). Take the db element of $V V^\dagger = I$, for example, one has

$$V_{ud} V_{ub}^* + V_{cd} V_{cb}^* + V_{td} V_{tb}^* = 0. \quad (\text{A.7})$$

The usual convention is to normalize by $A\lambda^3$, then $V_{cd} V_{cb}^*/A\lambda^3 \cong -1$, and $V_{ud} V_{ub}^*/A\lambda^3 \cong \rho + i\eta$ (for our purpose, let us not distinguish between $\bar{\rho} + i\bar{\eta}$ and $\rho + i\eta$), and $V_{td} V_{tb}^*/A\lambda^3$ follows by unitarity. Equation (A.7) is represented by the regular triangle to the left in Fig. A.2.

For the sb element of $V V^\dagger = I$, one has

$$V_{us} V_{ub}^* + V_{cs} V_{cb}^* + V_{ts} V_{tb}^* = 0. \quad (\text{A.8})$$

If one represents this in the same plot as (A.7), one notes that $V_{ud} V_{ub}^*/A\lambda^3 \cong \rho + i\eta$ is replaced by $V_{us} V_{ub}^*/A\lambda^3 \cong \lambda(\rho + i\eta)$ or the corresponding side has shrunk by

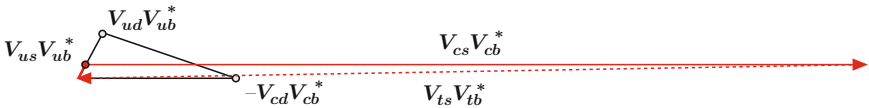


Fig. A.2 Geometric representations of (A.7) and (A.8), the latter being the long, *squashed* triangle. It is common to take the lower left point as the origin

$\lambda \cong 0.22$ in length. At the same time, $V_{cd}V_{cb}^*/A\lambda^3 \cong -1$ becomes $V_{cs}V_{cb}^*/A\lambda^3 \cong +1/\lambda$, which is now extended by $1/\lambda$ times and positive. It is represented by the long horizontal solid line extending to the right. Again, $V_{ts}V_{tb}^*/A\lambda^3$ follows by unitarity, which is represented by the slightly slanted dotted line pointing left (back to the “origin”). Thus, (A.8) is represented by the rather squashed and elongated triangle in Fig. A.2.

A.2 Illustration: Direct CP Violation

Direct CPV (DCPV), which has recently been established in $B^0 \rightarrow K^+\pi^-$ decay, gives the most intuitive illustration of Sect. A.1. That is, we have $f = K^+\pi^-$ in (A.2). Experimentally, the measurement of DCPV in $B^0 \rightarrow K^+\pi^-$ decay is the most straightforward, being just a counting experiment. One simply counts the difference between the number of events in $K^-\pi^+$ and $K^+\pi^-$ final states, with $m_{K\pi}$ reconstructing to m_{B^0} and with background under control. It is a matter of waiting for enough statistics. This is also a so-called self-tagged mode, since the charge of the K^\pm points back to the decaying particle being a B^0 or a \bar{B}^0 .

In Fig. A.3, we show the leading tree (T) and penguin (P) diagrams for $B^0 \rightarrow K^+\pi^-$ decay. Reading off from (A.3), one can readily see that the tree $b \rightarrow u\bar{s}u$ diagram carries a weak phase $\phi_3 = \arg V_{us}V_{ub}^*$, while P is dominated by $V_{cs}V_{cb}^* \cong -V_{ts}V_{tb}^*$, which is practically real. If the T and P amplitudes develop a relative strong phase δ (some absorptive part in the amplitudes), the interference between T and P would lead to *direct* (i.e., in decay amplitude itself) CPV. Indeed, this was observed in 2004 [5, 6], and $\mathcal{A}_{B^0 \rightarrow K^+\pi^-} \equiv \mathcal{A}_{CP}(B^0 \rightarrow K^+\pi^-) \sim -10\%$ is not small, recalling that $|\varepsilon'/\varepsilon|$ is at the 10^{-6} level in the kaon system. This illustrates rather clearly (A.1) and (A.2), where, to good approximation, $a_1 = |P|$ and $a_2 = |T|$. Unfortunately, the strong phase difference δ is of hadronic nature, the computation of which is rather challenging, and theorists do not generally agree with each other.

The whimsical name of the “penguin” diagram is attributed to a bet by John Ellis 30 years ago. Let us not get deeper into the historical anecdote, but note that if one complains that Fig. A.3(b) bears no resemblance to a “penguin,” then neither

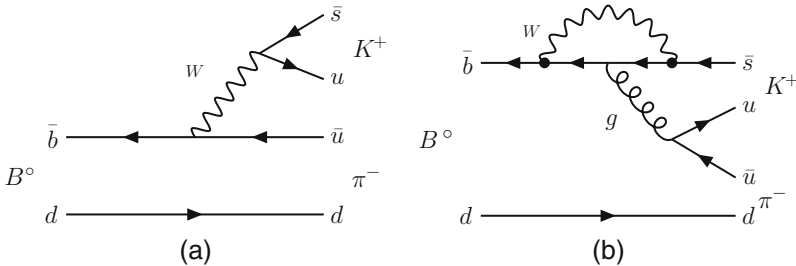


Fig. A.3 Tree and Penguin diagrams for $B^0 \rightarrow K^+\pi^-$ decay

does a Feynman diagram bear any resemblance to Feynman (although unlike the “penguin,” Feynman did pen it)!

A.3 Time-Dependent CP Violation

The idea for mixing- or time-dependent CP violation (TCPV) study at B factories is a beautiful one. Rather than derive the TCPV formalism [7], where we may get lost in the details, we give the formula and elucidate its content, thereby hopefully getting to appreciate some part of its beauty. In this way, we also prepare for the discussion of actual experimental studies in Chap. 2.

The TCPV asymmetry for $B^0 \rightarrow f$ decay, where f is a CP eigenstate, is

$$\begin{aligned} A_{\text{CP}}(\Delta t) &\equiv \frac{\Gamma(\bar{B}^0(\Delta t) \rightarrow f) - \Gamma(B^0(\Delta t) \rightarrow f)}{\Gamma(\bar{B}^0(\Delta t) \rightarrow f) + \Gamma(B^0(\Delta t) \rightarrow f)} \\ &= -\xi_f \mathcal{S}_f \sin \Delta m \Delta t + \mathcal{A}_f \cos \Delta m \Delta t. \end{aligned} \quad (\text{A.9})$$

The first part of (A.9) is defined quite analogous to (A.2), except that it is a little more delicate: $B^0(\Delta t)$ denotes the state at time Δt that evolved from a B^0 state at $\Delta t = 0$ and likewise for $\bar{B}^0(\Delta t)$. To avoid clutter and to compare better with (A.2) in a more transparent way, we have used a looser notation for what are actually differential decay rates (when conducting the analysis). Let us understand the second half of (A.9), where ξ_f is the CP eigenvalue of f , $\Delta m \equiv \Delta m_{B_d}$ and (BaBar uses $\mathcal{C}_f \equiv -\mathcal{A}_f$, i.e., picking up the initials for sine and cosine)

$$\mathcal{S}_f = \frac{2 \text{Im} \lambda_f}{|\lambda_f|^2 + 1}, \quad \mathcal{A}_f = \frac{|\lambda_f|^2 - 1}{|\lambda_f|^2 + 1}, \quad (\text{A.10})$$

are CPV coefficients, where λ_f is defined as

$$\lambda_f = \frac{q \langle f | S | \bar{B}^0 \rangle}{p \langle f | S | B^0 \rangle}. \quad (\text{A.11})$$

We see that λ_f depends on both B^0 – \bar{B}^0 mixing, i.e., $B_{H,L} = p B^0 \mp q \bar{B}^0$ (where H, L stands for the nominally “heavy” and “light” states) and decay to final state f . This is why TCPV is also called CPV in mixing–decay interference. The lifetime difference between the two neutral B mesons have been ignored to yield the simpler form of (A.9). This is a very good approximation for the B_d^0 – \bar{B}_d^0 system (but not so good for B_s^0 – \bar{B}_s^0 system, as will be touched upon in Chap. 2), so $q/p \cong e^{-2i\phi_1}$, hence $|q/p| \cong 1$. Using this last point, one can easily check that \mathcal{A}_f is nothing but the DCPV asymmetry in B^0 decay, hence this notation is more transparent than BaBar’s usage of \mathcal{C}_f .

For the golden $J/\psi K_S$ mode, the decay amplitude is real in the standard phase convention of (A.3), since it is dominated by the (color-suppressed) $b \rightarrow c\bar{c}s$ tree diagram, where $V_{cs}^* V_{cb}$ carries practically no weak phase. Thus,

$$\mathcal{S}_{J/\psi K_S} \cong \sin 2\phi_1, \quad \mathcal{A}_{J/\psi K_S} \cong 0, \quad (\text{A.12})$$

to very good accuracy. This is explained in Chap. 2. Many other $b \rightarrow (c\bar{c})_{\text{charmonium}}$ modes are also studied and correcting for ξ_f adds to the statistics.

Inspecting (A.2), (A.9), (A.10), and (A.12) altogether, one can now interpret (A.9) and gain some insight into the beauty and power of TCPV measurement, especially in the $J/\psi K^0$ mode (both $J/\psi K_S^0$ and $J/\psi K_L^0$). As stated, the $B^0 \rightarrow J/\psi K^0$ mode is dominated by a single decay amplitude, the color-suppressed $b \rightarrow c\bar{c}s$ tree diagram, with practically no weak phase in the decay amplitude. But there are two paths from an initial B^0 (i.e., B^0 at time $\Delta t = 0$) to decay to the $J/\psi K^0$ final state: a direct $B^0 \rightarrow J/\psi K^0$ decay or via B^0 oscillating to \bar{B}^0 , then $\bar{B}^0 \rightarrow J/\psi K^0$ decay. This corresponds to A_1 and A_2 of (A.2). As there is no CPV phase in either B^0 or \bar{B}^0 decay to $J/\psi K^0$, one is measuring the CPV phase in the B^0 to \bar{B}^0 oscillation amplitude. Here, the CP conserving phase is just the quantum mechanical time evolution phase $e^{i\Delta m\Delta t}$, which is *measured* experimentally. Thus, we measure the CPV phase factors \mathcal{S}_f and \mathcal{A}_f in the $\sin \Delta m\Delta t$ and $\cos \Delta m\Delta t$ oscillation coefficients when measuring the t -dependent asymmetries as defined in the first part of (A.9). The \mathcal{S}_f and \mathcal{A}_f corresponds to $\sin \phi$ in (A.2). With B^0 - \bar{B}^0 mixing dominated by the top quark, $S_{J/\psi K^0}$ measures a pure weak phase, and there is no ‘‘hadronic’’ or other ambiguity.

We stress that with ϕ_1 a fundamental, unique phase in the three-generation CKM matrix V , its measurement is as fundamental as determining the electromagnetic coupling constant α , the strong coupling constant α_s , or the Weinberg angle $\sin \theta_W$.

References

1. Kobayashi, M., Maskawa, T.: Prog. Theor. Phys. **49**, 652 (1973) 136
2. Yao, W.M., et al. [Particle Data Group]: J. Phys. G **33**, 1 (2006) 136, 137
3. Amsler, C., et al.: Phys. Lett. B **667**, 1 (2008); and <http://pdg.lbl.gov/> 136, 137
4. Wolfenstein, L.: Phys. Rev. Lett. **51**, 1945 (1983) 136
5. Aubert, B., et al. [BaBar Collaboration]: Phys. Rev. Lett. **93**, 131801 (2004) 138
6. Chao, Y., Chang, P., et al. [Belle Collaboration]: Phys. Rev. Lett. **93**, 191802 (2004) 138
7. Bigi, I.I.Y., Sanda, A.I.: Nucl. Phys. B **193**, 85 (1981) 139

Index

- $\mathcal{A}_{\text{CP}}(B^+ \rightarrow J/\psi K^+)$, 26, 126
 $\mathcal{A}_{\text{CP}}(b \rightarrow s\gamma)$, 82, 127
 Abelian flavor symmetry, 90
 $A_{\text{FB}}(B \rightarrow K^* \ell^+ \ell^-)$, 77–82, 126, 132
 Amplitude scan method, 39, 41
 Angular analysis, 50, 52, 82
 Artificial neural network (ANN), 51, 53
 Asymmetric beam energies, 8, 11, 12, 14, 87, 89

 $B^+ \rightarrow \tau^+ \nu_\tau$, 65–70, 83, 90, 96
 $B_s \rightarrow \mu^+ \mu^-$, 87, 90, 91
 $B_s \rightarrow \phi \mu^+ \mu^-$, 82
 Bag parameter, 7, 35
 Baryogenesis, 115, 129, 130
 Baryon Asymmetry of the Universe (BAU), 11, 115, 127–133
 Baryon number violation (BNV), 115, 119, 120, 123, 128
 $b \rightarrow c\tau\nu_\tau$ ($B \rightarrow \tau\nu_\tau + X$), 64, 65
 $B_d^0\text{--}\bar{B}_d^0$ mixing, 5, 7, 12, 76, 101, 139, 140
 $B_s^0\text{--}\bar{B}_s^0$ mixing, 33–43, 50, 54, 81, 101, 126, 137
 $B \rightarrow D^{(*)}\tau\nu_\tau$, 68–70
 Beam-constrained mass M_{bc} , 19
 Belle detector, 14
 Beyond the Standard Model (BSM), 3, 4, 29, 33, 37, 45, 69, 78–81, 108, 109, 112–116, 123–125, 133, 137
 B factory, 3, 4, 7, 8, 12, 20, 27, 39, 58, 59, 61, 66–69, 76, 78, 79, 81, 83, 93, 95, 99, 101, 102, 104–106, 115, 118–121, 126, 127, 132, 133
 $b \rightarrow sg$, 64
 $b \rightarrow s\gamma$ ($B \rightarrow X_s\gamma$), 57–64, 68, 88, 126
 Big Bang, 128
 $B \rightarrow K + \text{nothing}$, 84, 85
 $B \rightarrow K^*\gamma$, 58, 87–90
 $B \rightarrow K^{(*)}\ell^+\ell^-$, 73–82

 $B \rightarrow K^{(*)}\nu\nu$, 82–85
 $B^+ \rightarrow J/\psi K^+$, 26–29, 91
 $B^0 \rightarrow \eta' K_S$, 16–18
 $B^0 \rightarrow \phi K_S$, 15–18
 $B^0 \rightarrow K_S^0 \pi^0 \gamma$, 87–90
 B–L conservation (violation), 120
 Box diagram, 6, 7, 25, 34, 35, 37, 43–49, 73, 74, 77, 82, 102, 109, 126, 129, 131
 $b \rightarrow s\ell^+\ell^-$, 73–78, 81
 $b \rightarrow s\nu\bar{\nu}$, 74, 75, 82
 BSM Higgs boson, 82–85, 87, 90, 91, 93, 95–99, 124

 Cabibbo-favored (CF), 103–105
 Cabibbo-suppressed (CS), 103
 Charged Higgs boson, 57–59, 90, 124
 CKM, 6–8, 11, 15, 25, 26, 29, 35–38, 42, 47, 68, 70, 78, 82, 102, 110, 124–128, 136, 140
 Color-suppressed tree (C), 24, 26, 28, 33, 126, 139
 Complex dynamics, 80, 135
 $\cos 2\Phi_{B_s}$, 43, 52
 CP violation (CPV), 2–7, 125, 126, 128–133, 135–140
 current conservation, 62, 75, 87

 $D_s^+ \rightarrow \ell^+ \nu_\ell$, 70, 71
 Dalitz analysis, 105, 106, 109
 Dark matter (DM), 82–85, 93, 96, 97, 99
 $D^0\text{--}\bar{D}^0$ mixing, 101–109, 130
 Decay constant, 7, 35, 42, 65, 68, 70, 90
 $\Delta\Gamma_{B_s}$, 43, 52, 53
 $\Delta\mathcal{A}_{K\pi}$ problem, 21–26, 29, 33, 46, 47, 49, 54, 80, 81, 125–127, 129, 132
 $\Delta\mathcal{S}$ problem, 11, 16–18, 26, 29, 33, 46, 47, 126, 132
 Direct CPV (DCPV), 11, 18–29, 82, 123, 126, 132, 138, 139
 DORIS, 8

- Doubly Cabibbo-suppressed (DCS), 103, 105, 106
- Electromagnetic calorimetry, 58, 67, 68, 113
- Electroweak penguin (P_{EW}), 24–26, 46, 48, 49, 73, 78, 82, 110, 113, 126, 129, 131
- Electroweak phase transition (EWPhT), 128, 129
- Electroweak precision tests (EWPT), 46, 131
- Electroweak symmetry breaking (EWSB), 1, 4, 75, 76, 123–125, 130
- Energy difference ΔE , 19
- Energy frontier, 4
- EPR coherence, 12
- ε_K , 110
- ε'/ε , 110, 114, 138
- Extra Dimensions, 117, 124
- Flavor changing neutral current (FCNC), 16, 29, 82, 91, 101, 124, 125, 128
- Flavor tagging, 13, 39, 40, 45, 51–53, 103, 109, 118
- Forward Detector, 95, 96
- Forward-backward asymmetry (A_{FB}), 73, 77–82, 126, 132
- Fourth generation, 25, 26, 28, 29, 46–50, 53, 54, 76, 81, 108, 113, 124–132
- Full reconstruction, 61, 66–69, 83, 93, 96
- GIM mechanism, 7, 48, 49, 57, 109, 129
- Grand Unified Theory (GUT), 116, 117
- Grossman–Nir bound, 113
- Hermeticity, 83, 95, 96, 99
- Hierarchy problem, 124
- Higgs affinity, Yukawa coupling, 6, 46, 48, 66, 74, 84, 102, 129, 130
- Higgs boson, 1, 84, 85, 96, 97, 130
- HyperCP events, 84, 95, 97, 99
- Inami–Lim functions, 48, 109
- International Linear Collider (ILC), 1, 4, 97, 131
- IP (beam) profile, 89, 103
- J-PARC, 113
- Jarlskog Invariant, 128–130
- $K^+ \rightarrow \pi^+ \nu \bar{\nu}$, 109–114
- $K_L \rightarrow \pi^0 \nu \bar{\nu}$, 112–114, 127
- K-short (K_S) vertexing, 89, 103
- $K \rightarrow \pi \mu^\pm e^\mp$, 116, 117
- Kaluza–Klein excitations, 124
- KEKB, 12–15, 95
- Kobayashi and Maskawa (KM), 5, 7, 8, 125, 127–130, 133, 136
- K^0 - \bar{K}^0 mixing, 7, 101
- Large fluctuations, 16
- Large Hadron Collider (LHC), 1–4, 33, 37, 40, 44, 45, 49, 63, 68, 76, 79, 81, 82, 84, 85, 87, 89–91, 93, 96, 97, 99, 109, 119, 123, 126, 131–133
- LEP, 34, 46, 64, 96, 131
- Leptogenesis, 115, 118, 124
- Lepton charge asymmetry A_{SL} , 43
- Lepton flavor violation (LFV), 115–119
- Lepton number conservation, 116
- Little Higgs, 125
- Loops, 1, 6, 7, 16, 37, 46–48, 54, 57, 62, 73–78, 83, 84, 93, 102, 108, 115–117, 121, 129, 133
- Luminosity frontier, 3
- Minimal Flavor Violation (MFV), 79
- Minimum ionizing particle (MIP), 95, 96
- Mixing-decay interference, 139
- $\mu \rightarrow e\gamma$, 115–117
- Muon $g - 2$, 118
- Nambu–Jona-Lasinio model, 130
- Neutrino counting, 46, 131
- Neutrino mixing (oscillation), 115, 116, 124
- New Physics (NP), 4, 8, 11, 16, 17, 21, 23–26, 33, 39, 43, 49, 58, 59, 61, 62, 64–66, 70, 77, 79, 81, 87, 88, 93, 99, 101, 102, 108, 109, 112, 113, 123, 124, 126, 127, 129, 131–133
- Next-to-next-to-leading order (NNLO), 57, 60–63, 88
- Nondecoupling, 6–8, 25, 46–49, 54, 61, 73, 74, 76, 77, 113, 126, 129, 131
- ν_μ – ν_τ mixing, 117
- Opposite side tagging (OST), 39, 40, 51
- Oscillation probability, 38
- Partial reconstruction, 58
- Particle identification (PID), 13, 19–21, 40, 45
- PEP-II, 3, 7, 12–15, 95
- Perturbative QCD factorization (PQCD), 19, 24, 25, 47, 126
- Photon energy cut, 59–61
- Photonic penguin, 73–75, 77
- Polarization in $B \rightarrow VV$, 29
- PSI, 12, 116
- QCD factorization (QCDF), 20, 24

- R-parity violating SUSY, 90
- Radiative return (ISR), 93
- Rare B reconstruction, 19
- Right-handed (RH) interactions, 87–89, 124

- Sakharov conditions, 11, 128
- Same side tagging (SST), 40, 51, 103
- Self-tagging, 19, 138
- Semileptonic B_s^0 decay, 38–40
- S_f, A_f , 12, 15–17, 139, 140
- $\Sigma^+ \rightarrow p\mu^+\mu^-$, 97
- $\sin 2\beta/\phi_1$, 4, 5, 7, 13, 15, 16, 33, 37, 50, 136, 139, 140
- $\sin 2\phi_{B_s}$, 33, 37, 38, 43–54, 81, 125–127, 130, 132, 133
- Slepton mixing, 116–118
- Soft Collinear Effective Theory (SCET), 25
- Spontaneous symmetry breaking, 6, 75, 133
- Squark mixing, 15, 16, 35, 37, 90
- Standard Model (SM), 1, 5, 136
- Strong penguin amplitude (P), 15, 21–25, 48, 73, 138
- Strong phase, 21–29, 50, 52, 53, 105, 106, 109, 135, 138
- Super B factory, 3, 4, 18, 61, 63, 68, 70, 76, 79, 82, 83, 86, 87, 89, 96, 99, 109, 119, 127, 132, 133
- Supersymmetry (SUSY), 16, 25, 34, 46, 54, 57, 61–63, 65, 89–91, 96–98, 116–118, 123, 124
- Systematic error, 21, 27, 28, 61, 70, 71

- Tagged $B_s^0 \rightarrow J/\psi\phi$, 44, 50–54, 125, 126, 132, 133
- $\tan\beta$, 59, 62–69, 87, 90, 118
- Tau/charm factory, 101, 115, 118
- $\tau \rightarrow \bar{p}\pi^0$, 119, 120
- $\tau \rightarrow \ell\ell\ell^{(\prime)}$, 118, 119
- $\tau \rightarrow \ell\gamma$, 117–119

- $\tau^\pm \rightarrow \Lambda\pi^\pm$, 119, 120
- Tevatron, 3, 5, 20, 27–29, 33, 34, 36, 38, 40, 44, 45, 50, 54, 82, 91, 102, 104, 126, 131–133
- Time-dependent CPV (TCPV), 11, 13, 15, 23, 26, 50–54, 87–89, 104–106, 126, 127, 132, 139, 140
- Tree amplitude (T), 21, 23, 71, 126, 138
- Two track vertex trigger, 40, 41

- Unitarity bound, 130, 132
- Unitarity quadrangle, 109, 127, 128, 130
- Unitarity triangle, 8, 29, 36, 37, 109, 125, 127–129, 137, 138
- Unparticle physics, 123
- Untagged $B_s^0 \rightarrow J/\psi\phi$, 43, 44
- $\Upsilon(1S) \rightarrow \gamma a_1^0$, 96–99
- $\Upsilon(nS)$ probes, 93–99
- $\Upsilon(1S) \rightarrow \text{nothing}$, 93–96

- Vacuum expectation value (v.e.v.), 1, 5, 7, 59, 62, 74, 76, 84, 87, 125, 129, 130
- Vector-like quark, 125

- Weak phases, 2, 11, 21, 24, 25, 28, 46, 59, 80–82, 108, 135, 138–140
- Weakly Interacting Massive Particle (WIMP), 84
- Width mixing, 37, 43, 52, 53, 101–109
- Wilczek process, 98
- Wilson coefficients, 47, 48, 78–82, 88
- Wolfenstein form, 36, 136, 137

- x_D , 103, 105–109, 126

- Z penguin, 73–78, 80, 82
- Z' model, 29, 54, 81, 82, 124
- $Z \rightarrow b\bar{b}$, 127